JTTEE5 10:255-266

Particle Temperature Measurement in the Thermal Spray Process

J.R. Fincke, D.C. Haggard, and W.D. Swank

(Submitted 14 February 2000)

Particle temperature is a fundamental parameter in the thermal spray process. The measurement of particle temperature usually relies on the measurement of the radiance of the hot, incandescent, particles in two or more wavelength or color bands. Measurement techniques can be categorized as single particle and ensemble methods. Single particle methods use high-speed pyrometry to estimate the temperature of individual particles. The mean and standard deviation of the particle temperature distribution can then be obtained from observations of sufficient numbers of individual particles. Ensemble methods observe large numbers of particles simultaneously and yield an estimated mean temperature directly, but cannot provide information on the shape or width of the particle temperature distribution. Both techniques have inherent errors, strengths, and limitations that are examined and discussed.

Keywords diagnostics, particle temperature

Introduction

In the thermal spray process, solid particles are injected into a high-temperature, high-velocity gas flow field. The intent is to melt the particulates and to subsequently deposit them onto a substrate. At impact, the particle temperature, molten fraction, size, and velocity along with substrate temperature and surface characteristics control the morphology of the individual particle splats. Particle temperature and mass flux control the rate at which a deposit is formed and influence the cooling and solidification rate. These factors, in turn, control the adhesion, strength, microstructure, and porosity of a coating. The in-flight measurement of particle parameters provides information, which is useful in the optimization of the coating process.

Particle temperature measurement can be characterized as single particle techniques where each particle is observed "one at a time" and ensemble techniques where the pyrometer observes an ensemble of particles simultaneously. Single particle techniques require that the particle measurement volume be limited and that the number of entrained particles (powder feed rate) be small enough that individual particles can be observed without overwhelming interference from other, nearby particles. Measurement volumes on the order of one mm^3 are not unusual.[1–4] Particle velocities in the thermal spray process are generally on the order of 100 to 500 m/s or even higher in some cases. This, coupled with the small measurement volume size, results in single particle observation times on the order of 1 to 10 μs, necessitating the use of relatively high-speed detectors and electronics with bandwidths on the order of 0.1 to 1 MHz or greater. Temperature data on a sufficient number of individual particles are required to ensure an adequate statistical representation of the mean and standard deviation of the ensemble. The acquisition of sufficient numbers of particles, typically several hundred and preferably several thousand, requires observation times of seconds to minutes depending on the rate of particle passage (particle flux) and the duty cycle or dead time inherent in the instrument. To characterize the entire (nonuniform temperature) particle flow field, the small measurement volume must be moved relative to the spray pattern and the spatial distribution of particle temperature mapped. Temperature differences of several hundred degrees from the top to the bottom of the spray pattern typically exist. The spatial variation in temperature is due to differences in the trajectory of the particles relative to the gas flow field and due to aerodynamic particle sizing, where the larger particles have trajectories somewhat different than that of the smaller particles.[1,2] For a fixed measurement volume location, movement of the spray pattern relative to the measurement volume results in an apparent change in particle temperature due to the observation of a different region of the spray pattern. Spray pattern position is a function of particle size distribution, injection velocity and direction, and gun power and gas flow rates. Thus, in control applications, where operating parameters are changing and a small, fixed position measurement volume is used, care must be taken to ensure that apparent changes in temperature are real and not due to spatial movement of the spray pattern relative to the measurement volume.

Ensemble measurement techniques do not attempt to distinguish between individual particles and, in fact, are designed to observe relatively large measurement volumes containing relatively large numbers of particles at a given time. The measurement volume generally consists of an approximately cylindrical chord through the spray pattern. This chord is preferably oriented in the plane of the injector so that the measurement is insensitive to movement of the spray pattern relative to the measurement volume. Ensemble techniques are not restricted to lightly loaded thermal spray processes and work equally well for heavily loaded high-velocity oxygen fuel (HVOF) and high-powered plasma spray processes, where single-particle techniques are not able to distinguish between individual particles. That is, as the rate of powder injection increases, the probability of observing a single, isolated particle in the measurement vol-

J.R. Fincke, D.C. Haggard, and **W.D. Swank,** Idaho National Engineering and Environmental Laboratory, Idaho Falls, ID 83415-2211. Contact e-mail: jf1@inel.gov.

ume sharply decreases. Ensemble techniques yield an estimate of mean particle temperature only.

Both ensemble and single-particle techniques have strengths and limitations and are individually suited for different applications. Both techniques suffer from the fundamental problem inherent in all optical temperature measurement techniques: the fact that the spectral emissivity is generally not well known, can change due to surface oxidation or other chemical reactions, and is generally a (unknown) function of temperature. In the discussion that follows, prior work on the development of in-flight particle temperature measurement techniques, with special emphasis on the thermal spray process, will be reviewed. The errors associated with unknown or changing emissivities and the inherent problems, strengths, and weaknesses of both single particle and ensemble methods will be examined along with the sources of and realistic estimates of measurement uncertainty.

Historical Development

The in-flight measurement of the temperature of small particles has been successfully performed by a number of researchers. Gurevich and Shteinberg[5] described a two-color technique for measuring the temperature of burning droplets of liquid fuel as early as 1958. Later, Kruszewska and Lesinski[6] reported the first application of an absolute radiance technique to the measurement of single-particle temperature in a plasma torch. The sample volume consisted of a chord through the flow field, defined by the back projection of the optical systems limiting aperture through the imaging light collection optics. The technique was further developed by Vardelle *et al.*[7] and extended to a two color-technique by Mihsin *et al.*[8,9] Jorgensen and Zuiderwyk[10] investigated a similar technique applied to individual combusting particles. Because of the relatively large depth of the field of the optics used, the measurement volumes were roughly cylindrical and generally extended across the entire spray pattern. Vardelle [*et al.*][11] overcame the limitations of the chordal measurement volume by developing a coincidence technique. In this technique, the plasma is viewed by two optical systems arranged perpendicular to each other. Each system with its aperture forms a region in space where a particle, when present, will produce a signal in the corresponding detector. The intersection of these two regions forms a localized measurement volume. By electronically restricting the data acquired to those instances where coincidence of signals in each detector is observed, the measurement volume size is consequently restricted.

Subsequent work enhanced the basic technique of single particle temperature measurement by the incorporation of a laser as a particle illumination source. Observing the laser beam at an angle restricts measurement volume size. The intersection of the laser beam with the chordal measurement volume defined by the instrument collection optics determines the measurement volume. Optics and apertures can be chosen to define measurement volumes of arbitrary size. In Ref 12, single particle temperature measurement was integrated with laser scattering for the simultaneous measurement of particle size and temperature. This same idea was extended to the simultaneous measurement of particle, size, velocity, and temperature by integration with laser Doppler velocimetry and laser scattering[1,2] and later upgraded by integration with phase Doppler laser velocimetry. When a laser Doppler velocimeter (LDV) is incorporated, the crossing of the LDV laser beams defines the measurement volume. The integration with laser scattering, or with laser Doppler velocimetry, has the advantage that relatively cold particles, or very small particles, produce a signal from the laser illumination even though they may not have sufficient intrinsic radiance to be detected by the temperature measurement channels.[2] Subsequently, data on the velocity, size, and numbers of "cold" particles are acquired. These particles would be unaccounted for by measurement techniques based purely on the measurement of spectral radiance.

In spite of the inability to distinguish "cold" particles, measurement techniques based purely on the observation of spectral radiance or incandescent light emitted by the particles have gained favor for the simultaneous measurement of particle velocity and temperature in the thermal spray process. Particle size can also be estimated from the measurement of the absolute radiance emitted by a particle once the temperature is obtained. Simultaneous measurement of particle size, velocity, and temperature of combusting coal particles was demonstrated by Tichenor *et al.*[13] This technique used an image plane coded aperture to obtain particle size, a transit timing technique to determine velocity, and two-color pyrometry to determine temperature. The technique was demonstrated at temperatures up to 1660 K on 100 to 500 μm coal particles at flow velocities of less than 10 m/s. Sakuta and Boulos[14,15] have more recently applied a similar technique to induction plasmas for velocities up to 100 m/s. A variation on these techniques is now commercially available as the DPV-2000 and is becoming widely used in thermal spray research.[3,4] In this technique, the depth of field of the instrument optics and the limiting aperture generally define the measurement volume.

The ensemble measurement technique is not nearly as well represented in the literature. It is however, simpler; applicable to heavily loaded thermal spray applications such a observed in many HVOF processes; and, because the measurement volume is a chord through the spray field, the measurement is relatively insensitive to spatial movement of the spray pattern. The technique yields an estimate of mean particle temperature but cannot provide information on the statistical distribution of temperature. The insensitivity of the measurement technique to spatial movement of the spray pattern and response times that are generally significantly less than 1 s make the technique particularly attractive for application to monitoring and control in the manufacturing environment. The ensemble measurement technique has been applied to the thermal spray process since at least 1973.[16] The measurement technique, which is periodically rediscovered, 1988,[17] 1989,[18] 1995,[19] has been successfully incorporated into a closed-loop controller for the plasma spray process.[20,21]

Measurement Limitations

There are several fundamental limitations to the measurement of temperature in the thermal spray process. The first is that the particle temperature cannot be measured inside the luminous plasma (or combustion jet) core. The radiated power of the highly luminous plasma is much greater (brighter) than the light emitted by a small incandescent particle. Practically, for typical

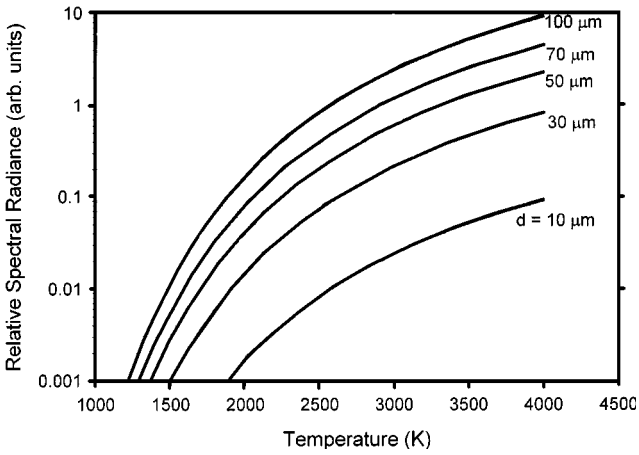

Fig. 1 Relative spectral radiance as a function of temperature and particle diameter at a wavelength of 900 nm

plasma spray conditions, this means that a particle's temperature cannot be readily obtained by measuring their emitted radiation any closer to the nozzle exit than about 50 mm.[9] The second limitation is that plasma light that is scattered by a particle, even after the particle has exited the hot core, can influence the measurement of temperature. Scattered light restricts the proximity to the plasma in which temperature measurements can be obtained and also determines the lower limit of the temperature that can be measured. Practically, for standoff distances on the order of 100 mm, the lower temperature measurement limit is around 1500 K.[9,22] A third limitation, which affects the single particle measurement technique, is the ability to observe the light emitted by a single particle without overwhelming interference from surrounding particles. For typical plasma spray conditions, with particle loading of a few kg/h, this condition is generally met. For many HVOF applications and high-power plasma spray situations, where the loading may be in excess of 10 kg/h, it is often impossible to distinguish single particles.

The exact limits imposed by the issues described above are dependent on the size and emissivity of the particles, the plasma gases and power level, the detectors and wavelengths used, and the particle feed rate. Obviously, for the same particle feed rate, there will be a factor of 1000 more particles if the average particle size is 10 μm rather than 100 μm. Hence, for the same feed rate, a powder with a relatively large average size may have few problems with multiple particles in the measurement volume at any instant in time, while a smaller average size powder may be plagued by the problem. Also, the particle size distribution along with temperature determines the dynamic range requirement of the measurement electronics. For most situations, a dynamic range of 1000 is probably sufficient. This is illustrated in Fig. 1. If the particles size distribution is between 10 and 70 μm, and the temperature ranges between 2000 and 4000 K, the required dynamic range is approximately 2000. This suggests that for a linear system the digitizers used to capture the signals should have a minimum dynamic range of 12 bits and 14 or 16 bits would be preferable.

The issues associated with multiple particles in the measurement volume are absent when the ensemble particle temperature measurement is used. The dynamic range requirement is also smaller. For a given particle size, the relative magnitude of the emitted radiation varies by a factor of 2 to 3 or so over a temperature range between 1000 and 4000 K. The ensemble method observes multiple particles in the measurement volume. For a fixed particle feed rate in kg/h, the number of particles in the measurement volume varies as $1/d^3$, where d is the particle mean diameter. The projected area of a particle linearly determines the magnitude of the radiated power of a single particle and is proportional to d^2. For a given particle feed rate, the total projected area of the particle ensemble observed varies as $1/d$ for variations in particle size. Hence, a smaller mean particle diameter actually decreases the required dynamic range of the ensemble measurement.

Calibration and Emissivity Correction

The basic premise behind all radiation thermometry is Plank's law, which describes the emissive power of a radiating body as a function of wavelength, emissivity, and temperature. Planck's law is

$$i_\lambda = \frac{c_1 \varepsilon_\lambda \Delta\lambda \Omega A_p}{\lambda^5 \left(e^{c_2/\lambda T} - 1\right)}$$

where T is the surface temperature of the radiating body, $c_1 = 0.595 \times 10^{-12}$ W/cm^2 and $c_2 = 1.4388$ (cm)(K) are constants, ε_λ is the spectral emissivity, A_p is the area of the emitter, Ω is the solid angle of the light collection optics, and η is the spectral bandwidth. Dual-wavelength (ratio or two-color) pyrometry involves the measurement of the spectral energy in two different wavelength bands. Using Planck's law, the ratio of radiant energy, R, in two different wavelength bands, λ_1 and λ_2, is given by

$$R = \frac{\varepsilon_{\lambda_1}}{\varepsilon_{\lambda_2}} \left(\frac{\lambda_2}{\lambda_1}\right)^5 \exp\left[\frac{c_2}{T}\left(\frac{1}{\lambda_2} - \frac{1}{\lambda_1}\right)\right]$$

where Wein's formula valid for $\exp\left(\frac{c_2}{\lambda T}\right) >> 1$ has been used.

In measurement systems, the ratio of the observed signal associated with each wavelength is

$$R_2 = \frac{k_{\lambda_1}}{k_{\lambda_2}} \frac{\varepsilon_{\lambda_1}}{\varepsilon_{\lambda_2}} \left(\frac{\lambda_2}{\lambda_1}\right)^5 \exp\left[\frac{c_2}{T}\left(\frac{1}{\lambda_2} - \frac{1}{\lambda_1}\right)\right]$$

where the ration $k_{\lambda_1}/k_{\lambda_2}$ is the ratio of detector responsivity and optical efficiencies at the two wavelengths used. This relationship is common to both single particle and ensemble measurement methods.

By using the ratio, the measurement is insensitive to the absolute magnitude of radiation falling on the detector and the field of view need not be filled. The use of the ratio of two signals means that a relative calibration, rather than a more difficult absolute calibration, is required and that the projected area of the particles(s) disappears from the result when the ratio is formed. The technique, however, is susceptible to errors caused by variations in emissivity with wavelength and special precautions must be observed to ensure that adequate signal strength (signal-to-noise ratio) is available to obtain an accurate measurement. In practice, the particles are often assumed to be gray body radia-

tors, that is, the emissivities can differ from that of a blackbody, $\varepsilon_b = 1$, but are equal for the two wavelengths chosen, $\varepsilon_{\lambda_1} \equiv \varepsilon_{\lambda_2}$. Under this assumption, the ratio of emissivities is unity. In fact, the spectral emissivities generally differ significantly from the gray body assumption. Additionally, emissivities are not well known for many materials, can change due to surface oxidation or other chemical reactions, and exhibit a (generally unknown) dependence on temperature. In the following, we will briefly examine the magnitude of the potential errors associated with the gray body assumption.

The calibration of high-temperature radiation pyrometers is often performed using a tungsten lamp as the calibration source. The actual materials sprayed range from pure metals, alloys, intermetallics, and refractories, to various ceramics, including special composite materials, which can consist of oxides, carbides, or other compounds in a metal matrix. The melting point of common coating materials ranges from around 1600 K for stainless steel to around 3000 K for zirconia, and as high as ≈3600 K for tungsten. Tungsten ribbon lamp calibration sources are capable of temperatures to 2800 K, a range that reasonably covers the temperatures encountered for most common coating materials. Tungsten is not a gray body radiator.[23] At a temperature of 2000 K, the spectral emissivity of tungsten varies from 0.42 at 800 nm to 0.314 at 1.35 μm. The ratio of emissivities at two common pyrometer wavelength pairs is $\frac{\varepsilon_{\lambda 1}}{\varepsilon_{\lambda 2}} = 1.09$ for $\lambda_1 = 700$ nm, $\lambda_2 = 850$ nm, and $\frac{\varepsilon_{\lambda_1}}{\varepsilon_{\lambda_2}} = 1.23$ for $\lambda_1 = 950$ nm, $\lambda_2 = 1.35$ μm. Many metallic materials such as nickel, stainless steel, and inconel have a spectral emissivity ratio that is similar, though not identical, to that of tungsten.[23,24] Many metal oxides and ceramics behave more like gray bodies, *i.e.*, their spectral emissivity ratio is close to unity.[25]

The problem is basically one of how to infer the true temperature from the radiant energy sensed by the instrument. If the relationship between emissivity and wavelength is known, it is possible to estimate a correction to the apparent temperature derived from the tungsten lamp calibration curve. The difference between the temperature indicated using the tungsten source calibration, T_w, and the true temperature, T_x, of a material whose spectral emissivity ratio differs from that of tungsten is found by setting the ratio of emissive powers for material x equal to that of tungsten, w, to arrive at

$$\frac{1}{T_x} = \frac{1}{T_w} + \frac{1n\left(\left.\frac{\varepsilon_{\lambda_1}}{\varepsilon_{\lambda_2}}\right|_x \left.\frac{\varepsilon_{\lambda_2}}{\varepsilon_{\lambda_1}}\right|_w\right)}{c_2\left(\frac{1}{\lambda_1} - \frac{1}{\lambda_2}\right)}$$

Figure 2 and 3 contain estimates of the true and apparent temperatures using the above equation for various emissivity ratios, including the gray body assumption when the instrument is calibrated using a tungsten source. Figure 2 uses the wavelength pair $\lambda_1 = 700$ nm, $\lambda_2 = 850$ nm, while Fig. 3 uses the wavelength pair $\lambda_1 = 950$ nm, $\lambda_2 = 1.35$ μm. The corresponding errors, expressed in percent of reading, appear in Fig. 4 and 5. The apparent or color temperature is plotted on the abscissa, while the true temperature is plotted on the ordinate. The gray body assumption results in the largest discrepancy increasing from less than 50 K at temperatures less than 1500 K to as much as 600 K at

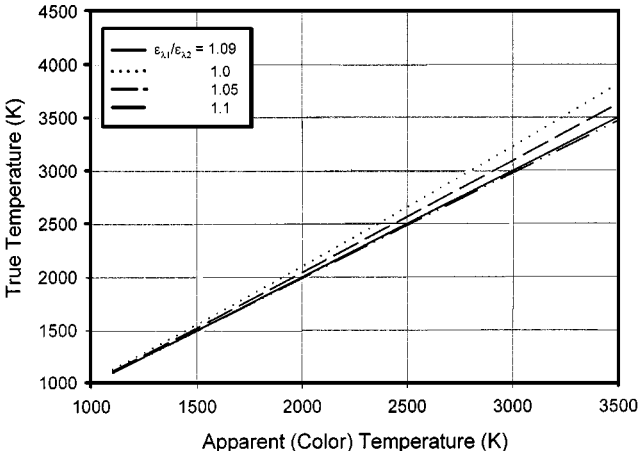

Fig. 2 Actual or "true" temperature as a function of apparent or "color" temperature and actual emissivity when calibration is performed using a tungsten lamp. The wavelength pairs are 700 and 850 nm

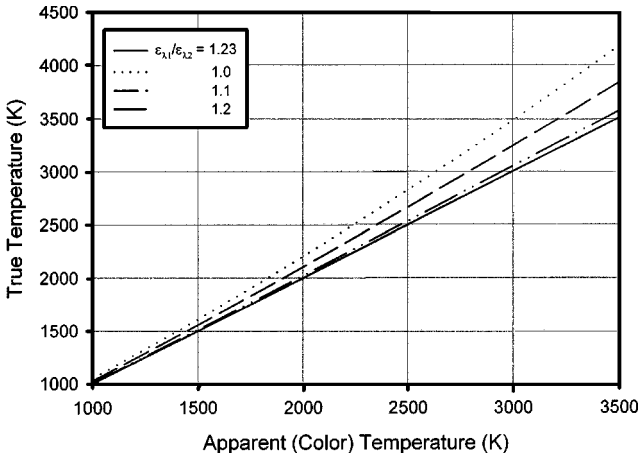

Fig. 3 Actual or true temperature as a function of apparent or color temperature and actual emissivity when calibration is performed using a tungsten lamp. The wavelength pairs are 950 and 1350 nm

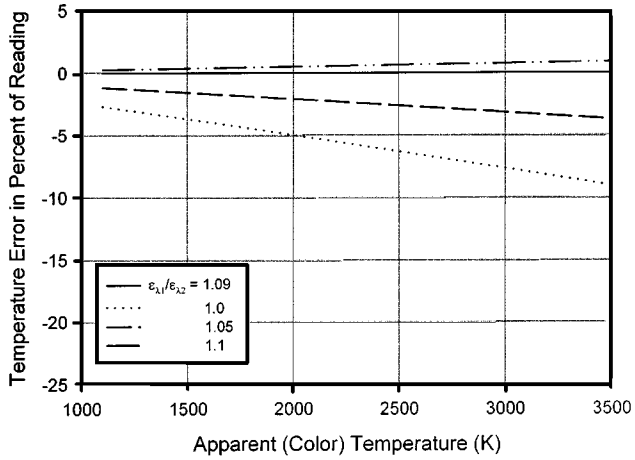

Fig. 4 Temperature measurement error in percent of reading corresponding to the results of Fig. 2. The wavelength pairs are 950 and 1.35 μm

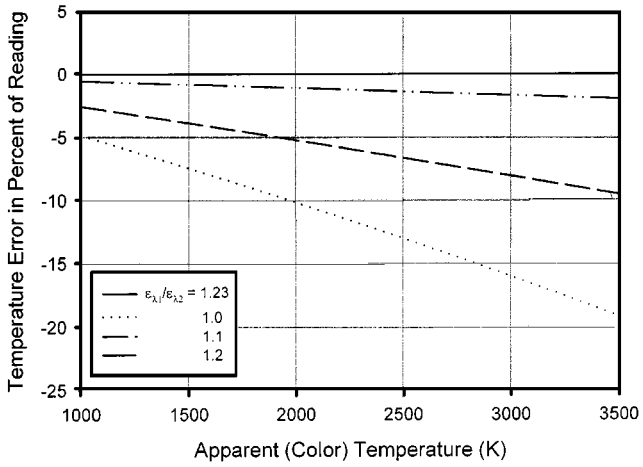

Fig. 5 Temperature measurement error in percent of reading corresponding to the results of Fig. 3. The wavelength pairs are 950 and 1.35 μm

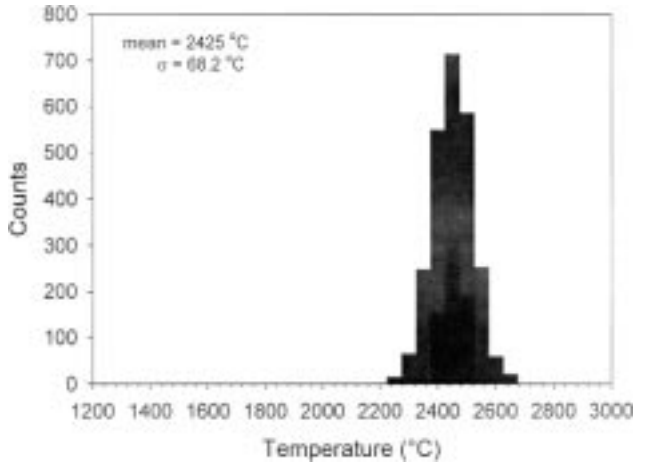

Fig. 6 Apparent temperature distribution due to the statistical response of the single particle temperature measurement system

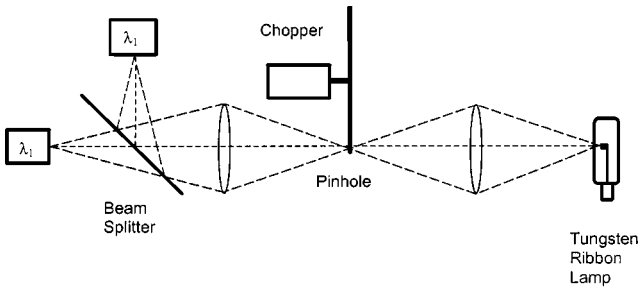

Fig. 7 Schematic of a particle simulating tungsten lamp calibration apparatus

3500 K (Fig. 3). That is, if the instrument using the wavelength pair $\lambda_1 = 950$ nm, $\lambda_2 = 1.35$ μm is calibrated using a tungsten lamp and reads 3500 K and if the observed particles are in fact gray body emitters, their actual temperature is around 4100 K. Under these conditions, the particle temperature is underestimated by as much as 600 K.

For applications where the absolute measurement of temperature is not required, such as controlling about a set point, or determining relative changes about a known condition, an emissivity correction may not be necessary. The temperature indicated will be single valued for a given particle temperature. That is, even if the spectral emissivity relationship is not known, and is not accounted for, the desired condition can be repeated by "setting" the spray device to produce particles that yield the same temperature reading. For example, an increase in particle feed rate may require an increase in operating power to produce a particle stream at the desired temperature condition. Another application would consist of maintaining the particle temperature within a quality control operating window. In this case, the absolute measurement of temperature may not be necessary. Since the major concerns are the ability to repeat a condition and compensate for drift from that condition. If a quality control set point has already been determined, then the measurement can be used without emissivity compensation to ensure that this set point is maintained. The accurate determination of absolute temperature, however, requires that the spectral emissivities of the calibration source and the departure of the particle from gray body behavior be accounted for.

Single Particle Temperature Measurement

As was correctly pointed out in Ref 9, the measurement of single-particle temperature is a statistical measurement. The statistical error is in addition to the "fixed" errors associated with calibration, emissivity, and long-term drift. Statistical errors arise from the statistical response of real measurement systems and are largely due to random signal fluctuations or noise; however other sources exist. These additional sources can be due to the location of the particle in the measurement volume, for instance. Because of vignetting, chromatic (and sometimes spherical) aberrations, or limited depth of field of the optical system, the spectral radiant power delivered to a detector may change due to the actual location of the particles, even if the particles have uniform temperature. Thus, this source of measurement error is also random, because the location of an individual particle in the measurement volume is random. This uncertainty is largely avoided by systems that use laser illumination to define the measurement volume, and can be minimized by the use of "well-corrected" optics in other systems. Random signal fluctuations result in the observed temperature having an apparent distribution width or standard deviation, even if the particles are monodisperse and have uniform emissivity and temperature.

The actual statistical performance of a measurement system is illustrated in Fig. 6. These data were generated using the tungsten lamp calibration apparatus, shown in Fig. 7. This system simulates a stream of particles at a given temperature using a calibrated tungsten ribbon lamp and a chopper with a pinhole drilled in its periphery. The high-speed chopper simulates the velocity, or passage of particles through the measurement volume, and the tungsten ribbon lamp produces a steady source of radiation characteristic of the emissivity and temperature of the tungsten ribbon. The detectors are photomultipliers and the wavelength bands are $\lambda_1 = 700$ nm, $\lambda_2 = 850$ nm. The digitizers have 12-bit resolution and the signal is ranged to use all 12 bits at a lamp temperature of 2800 °C. The random uncertainty in the measurement is $\sigma_I = 68$ °C at a mean temperature of 2430 °C.

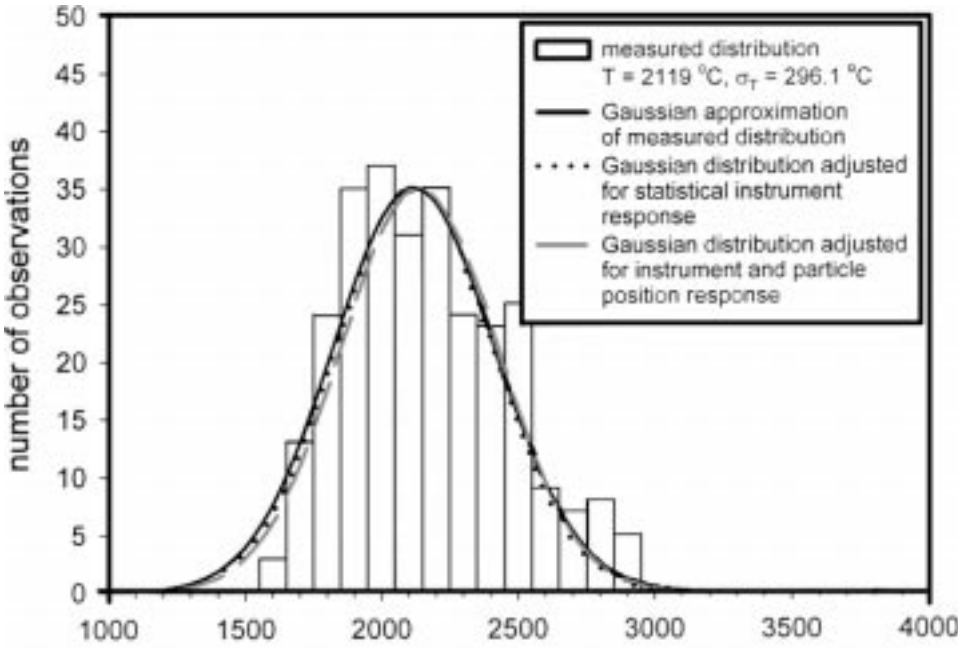

Fig. 8 Measured distribution of particle temperature with superimposed Gaussian distribution and distribution adjusted for statistical instrument response and particle position in the measurement volume

The shape of the distribution representing the instrument statistical response is approximately Gaussian. The measured particle temperature distribution therefore will be artificially broadened by the instrument statistical response. If the measured particle temperature distribution is also approximately Gaussian, then the actual standard deviation of particle temperatures, σ_a, will be related to the measured value, ξ_m, and the inherent instrument broadening, σ_I, by $\sigma_a^2 = \sigma_m^2 - \sigma_I^2$. This is illustrated in Fig. 8 on an actual measured distribution of particle temperatures. The sprayed material is nominally 50 μm NiCrAlY. The measured mean temperature is 2119 °C and the standard deviation is 296 °C. Shown in the figure is the measured distribution and a Gaussian distribution with the same mean and standard deviation as the measured distribution superimposed (solid line). Also shown is the Gaussian approximation adjusted for the statistical response of the instrument (dotted line). The mean temperature remains unchanged and the distribution is slightly narrowed. Also included in the figure is a third curve, which is adjusted for both the statistical instrument response and the uncertainty due to particle position in the measurement volume (gray line).

The component of statistical uncertainty due to particle position in the measurement volume is estimated in the following manner for our LDV based integrated particle size, velocity, and temperature instrument. The approach used to estimate the magnitude of the uncertainty is general, and the exact numerical values will depend on the specifics of a particular instrument. The crossing of the LDV laser beams defines the measurement volume. Using a small wire mounted on the rim of the chopper wheel to generate an LDV Doppler burst, the effective length of the measurement volume was obtained. This was measured to be approximately 0.8 or $\pm$0.4 mm about the midpoint. Next, the response of the instrument to the position of a particle in the measurement volume was obtained using the chopper configuration

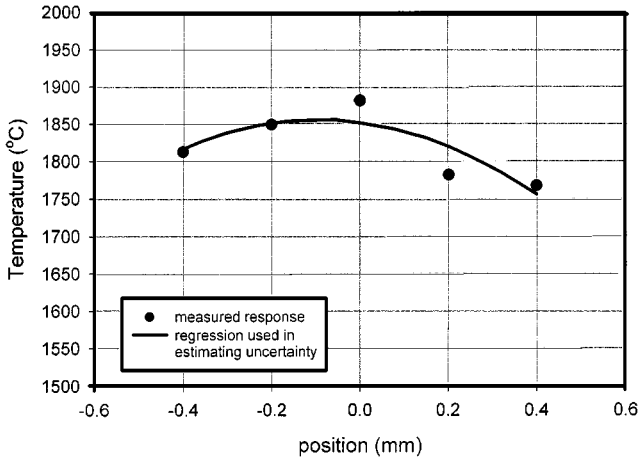

Fig. 9 Instrument temperature response as a function of particle position in the measurement volume

and particle simulating pinhole shown in Fig. 7. This was accomplished by mounting the calibration apparatus on a precision linear stage and placing the pinhole at various locations in the measurement volume. The data and the curve fit used to estimate the resulting particle temperature distribution are shown in Fig. 9. The resulting statistical distribution is estimated by assuming that particles are randomly and uniformly distributed in the meas-urement volume between $\pm$0.4 mm. For each particle location, a resulting mean particle temperature is measured. With the assumption that the location of the particles is uniformly distributed within the measurement, the corresponding probability of observing that temperature can then be obtained. The result appears in Fig. 10. Because of the shape of the temperature-position response curve (Fig. 9), the effect of particle position in

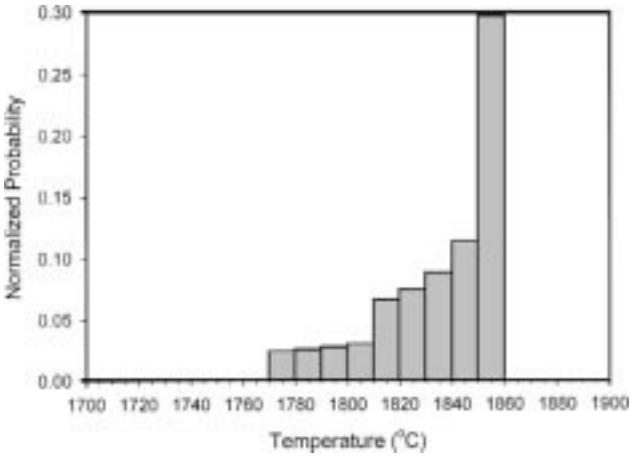

Fig. 10 Intrinsic statistical temperature distribution due to the location of the particle position in the measurement volume

the measurement volume biases the temperature distribution toward a value lower than the actual particle temperature. The actual particle temperature is 1855 °C, while the mean of the distribution in Fig. 10 is 1835 °C, a bias of approximately 0.8%. The standard deviation of the distribution is 22.7 °C and the third moment or "skewness," a measure of the asymmetry of the distribution, is −1.1, the negative sign indicating the bias toward a lower temperature. The corrected distribution is shown in Fig. 8, as the gray line. This correction, for the instrument analyzed, is small and barely discernable on the plot. The estimated uncertainty due to these two independent, random effects is approximated by the sum of the squares of the standard deviations, or ±71.9 °C.

Ensemble Particle Temperature Measurement

In the ensemble temperature measurement technique, a relatively large number of particles is simultaneously observed. This ensemble of particles is characterized by a distribution of particle size and particle temperature. The particle size and temperature may be correlated with the larger particles having, on average, a temperature lower than that of smaller particles.[1] A typical measurement volume size might be 5 mm in diameter and extend across the entire spray pattern;[19] hence, there may also be a spatial variation in particle temperature from one end of the measurement volume to the other. For a spray pattern with a spot size on the order of 40 mm, the resulting measurement volume is on the order of 1 cm^3. At typical powder loading of a few kg/h, the particle density is on the order of 100 to 1000 particles/cm^3,[1] resulting in the simultaneous observation of several hundred particles in the measurement volume at any instant in time. In estimating the response of the two-color pyrometer to the observed distribution of particle sizes and temperatures, it is assumed that the number of observed particles is large enough to avoid substantial statistical fluctuations in the mean and standard deviation and that the entire population is adequately represented in the measurement volume. It is also assumed that the distributions of size and temperature are approximately normal, and the mean temperature may depend on diameter in a linear fashion. Calculations indicate that over a wide range of particle sizes an approximately linear relationship between particle size and temperature is a reasonable assumption.[26] Under these conditions, the ensemble can be represented by a bivariate Gaussian distribution. Note that the smallest particles, due to their high velocities and limited residence times in the hot plasma, can actually be at a lower temperature than somewhat larger particles that have longer residence times. For zirconia powder under typical spray conditions, this divergence occurs at a particle size of approximately 20 μm.[26] Particles smaller than 20 μm can actually have a lower temperature than particles that are slightly larger than 20 μm. This effect is dependent on the specific material being sprayed and on operating parameters; hence, we will not attempt to account for this observation in the analysis of pyrometer response. By not doing so, the results represent a worse case estimate of the associated errors. In the following, the expected instrument response to the statistical and spatial distributions of particle sizes and temperatures will be calculated and compared to the true mean temperatures.

Assume that the size distribution of the ensemble of particles is adequately approximated by a normal distribution,

$$f_d(d_p) = \frac{1}{\sigma_d\sqrt{2\pi}}\exp\left[-\frac{(d_p - d_m)^2}{2\sigma_d^2}\right]$$

where d_m and σ_d are the mean and standard deviation of the particle size distribution, respectively. Assume also that for a given particle size the temperature distribution is also normal and that the particle temperature may be linearly correlated with particle size. Under these assumptions, the probability density function for the particle ensemble is given by the bivariate Gaussian or normal distribution

$$f(d_p, T) = \left(\frac{1}{\sigma_d\sqrt{2\pi}}\exp\left[-\frac{(d_p - d_m)^2}{2\sigma_d^2}\right]\right) \left(\frac{1}{\sigma_T\sqrt{1-\rho^2}\sqrt{2\pi}}\exp\left[-\frac{(T-b)^2}{2\sigma_T^2(1-\rho^2)}\right]\right)$$

where

$$b = \mu_T + \rho\frac{\sigma_T}{\sigma_d}(d_p - d_m)$$

and μ_T is the mean particle temperature, σ_T is the standard deviation of particle temperature, and ρ is a parameter describing the degree of the correlation between temperature and diameter. The right-hand side of the probability density function (PDF) is the conditional PDF of temperature *T*, given that the particle diameter is d_p. That is, the conditional PDF of *T* is itself normal with mean $\mu_T + \rho\frac{\sigma_T}{\sigma_d}(d_p - d_m)$ and variance $\sigma_T^2(1-\rho^2)$. Thus, with a bivariate normal distribution, the conditional mean of temperature, for a given diameter d_p, is

$$E(T|d_p) = \mu_T + \rho\frac{\sigma_T}{\sigma_d}(d_p - d_m)$$

For a given ensemble mean temperature, μ_T, correlation coefficient, ρ, and standard deviations of temperature and diameter, σ_T and σ_d, this equation defines the relationship between mean particle size and mean temperature. For $\rho = 0$, the distri-

butions of temperature and diameter are independent and uncorrelated; for $\rho \neq 0$, the mean particle temperature, as a function of diameter, is given by

$$T_m(d_p) = \mu_T + b(d_p - d_m)$$

where

$$b = \rho \frac{\sigma_d}{\sigma_T}$$

The response of a two-color pyrometer is estimated as follows. As before, the intensity of light incident on the collection optics, emitted by a particle of diameter d_p, with temperature T, and emissivity $\varepsilon(\lambda)$, in a narrow wavelength interval is given by

$$I(\lambda) = \frac{c_1 \varepsilon_\lambda \Delta\lambda \Omega \pi \frac{d_p^2}{4}}{\lambda^5 \left(e^{\frac{c_2}{\lambda T}} - 1 \right)}$$

For many particles in the measurement volume, the relative intensity observed by a detector in the wavelength interval $\Delta\lambda$ is given by

$$\bar{I}_\lambda = \int_{d_{\min}}^{d_{\max}} \int_{T_{\min}}^{T_{\max}} I(\lambda, d_p, T) f(d_p, T) dT\, dd_p$$

The intensity is assumed to be independent of particle velocity. The justification for this is as follows. For a measurement volume of spatial extent l_m, parallel to the particle velocity vector, the observation time for a particular particle i with corresponding diameter and velocity is $\tau_i = l_m/u_i$. The radiant energy emitted by the particle that is deposited in the detector is proportional to τ_i. Hence, slower particles will have a longer dwell time in front of the detector and will be more heavily weighted. However, the rate of arrival of particles with velocity u_i is proportional to the product of their population or number density n_i and velocity, yielding the rate of arrival in the measurement volume R, $R = n_i u_i$. While slower particles have a longer residence time, their rate of arrival is less. The net result is that the power deposited in the detector by particles with velocity u_i is proportional to $\tau_i n = n_i u_i (l_m/u_i) = l_m n_i$, which is proportional to the particle density and is not weighted by their velocity.

In two-color pyrometry, the temperature is obtained from the ratio of intensities in each of the two wavelengths bands λ_1, λ_2

$$R_m = \frac{\bar{I}_{\lambda_1}}{\bar{I}_{\lambda_2}} = \frac{\int_{d_{\min}}^{d_{\max}} \int_{T_{\min}}^{T_{\max}} I(\lambda_1, d_p, T) f(d_p, T)\, dT\, dd_p}{\int_{d_{\min}}^{d_{\max}} \int_{T_{\min}}^{T_{\max}} I(\lambda_2, d_p, T) f(d_p, T)\, dT\, dd_p}$$

and the temperature is obtained from

$$T = \frac{c_2 \left(\frac{1}{\lambda_2} - \frac{1}{\lambda_1} \right)}{1n \left(R_m \frac{\varepsilon_{\lambda_2}}{\varepsilon_{\lambda_1}} \left(\frac{\lambda_1}{\lambda_2} \right)^5 \right)}$$

In the calculations and discussion that follow, the emissivity ratio is assumed to be unity. Errors associated with departures from gray body behavior can be found in an earlier section. The double integrals are evaluated numerically.

Figure 11 and 12 contain a summary of calculated instrument responses to an ensemble of particles, where the particle temperature is completely uncorrelated with particle diameter. The plots compare the calculated temperatures (Fig. 11) and the temperature error in percent of reading (Fig. 12), plotted against actual mean particle temperatures. The standard deviation or width of the temperature distribution is treated as a parameter. The errors increase with decreasing temperature and increasing standard deviation. The temperature is consistently overestimated because the spectral radiance is a nonlinear increasing function of temperature. Hence, the averaging implicit in the ensemble temperature measurement tends to over weight the higher temperature particles. Because the temperature and diameter are completely uncorrelated in this calculation, the distribution of particle diameters does affect the instrument response. For a particle ensemble that has no correlation between particle temperature and size, with mean temperature around 2400 K with a standard deviation of 300 °C, similar to the measured distribution in Fig. 6, the mean temperature can be overestimated by 7% of reading or approximately 150 °C. At 3000 K, approximately the melting point of zirconia, the expected error is 5% or less, even for relatively broad distributions of particle temperatures.

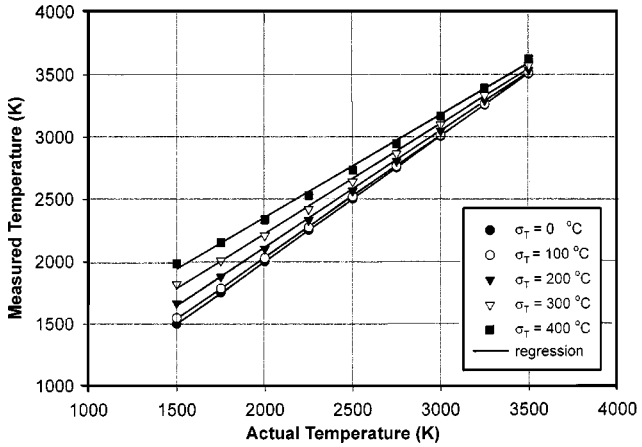

Fig. 11 Calculated pyrometer response to an ensemble of particles whose temperature and diameter are uncorrelated. Wavelengths are 950 nm and 1.35 μm

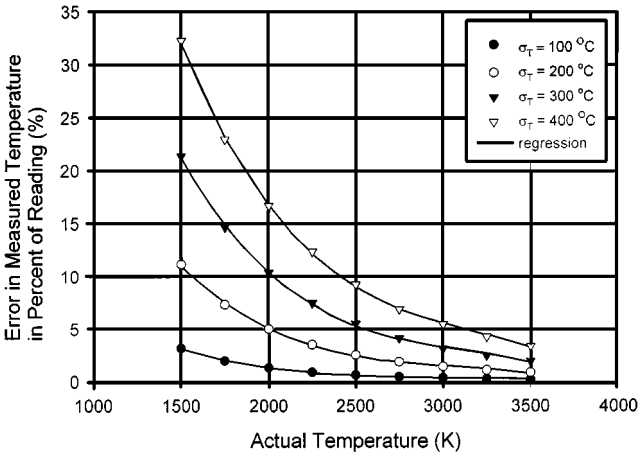

Fig. 12 Error in pyrometer response to an ensemble of particles whose temperature and diameter are uncorrelated. Wavelengths are 950 nm and 1.35 μm

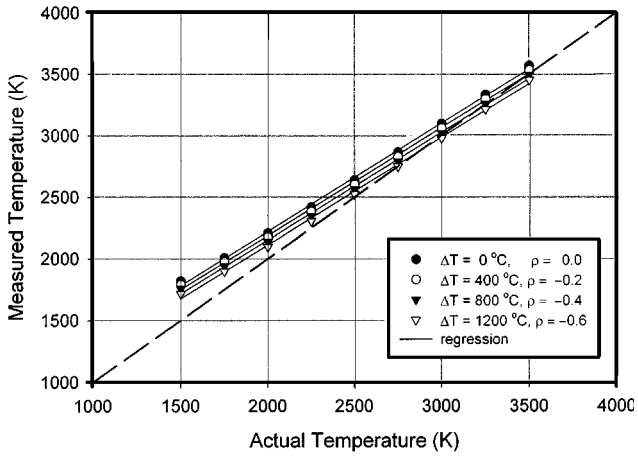

Fig. 13 Calculated pyrometer response to an ensemble of particles with $\sigma_T = 300$ K and $\sigma_d = 15$ μm and whose temperature and diameter are correlated

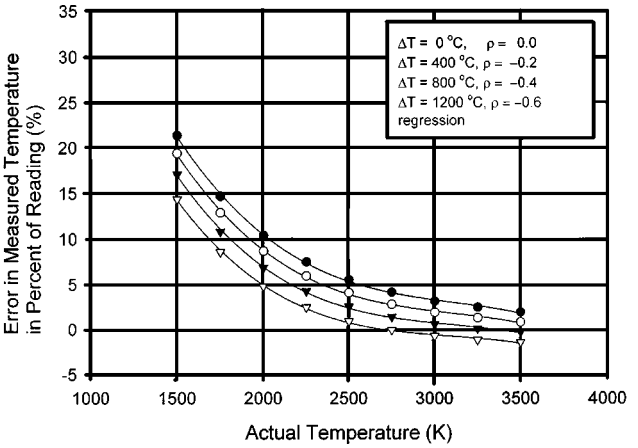

Fig. 14 Error in pyrometer response to an ensemble of particles with $\sigma_T = 300$ K and $\sigma_d = 15$ μm and whose temperature and diameter are correlated

The influence of the correlation between particle temperature and diameter is included by choosing ρ to be nonzero. If ρ is negative, the size and temperature are inversely correlated, with the smaller particles being at the higher temperatures. In performing the calculation, the mean temperature and diameter are specified, their standard deviation chosen, and the mean temperature difference between the smallest and largest particles assumed. For the calculation shown in Fig. 13 and 14, it is assumed that the mean particle diameter is 40 μm with a standard deviation of 15 μm. The mean temperature is a parameter and appears on the abscissa of the plot. The standard deviation of temperature is assumed to be 300 °C. The parameter ρ is chosen such that the range of mean temperatures (ΔT) between the largest (105 μm) and the smallest (5 μm) particles is between 0 and 1200 °C. The inverse correlation between particle temperature and particle size tends to reduce the error from that of the uncorrelated ensemble. The tendency for smaller particles to be at higher temperature increases their spectral radiance, while the decrease in their projected area (and subsequent weighting) is less, somewhat compensating for the tendency to over weight the hottest

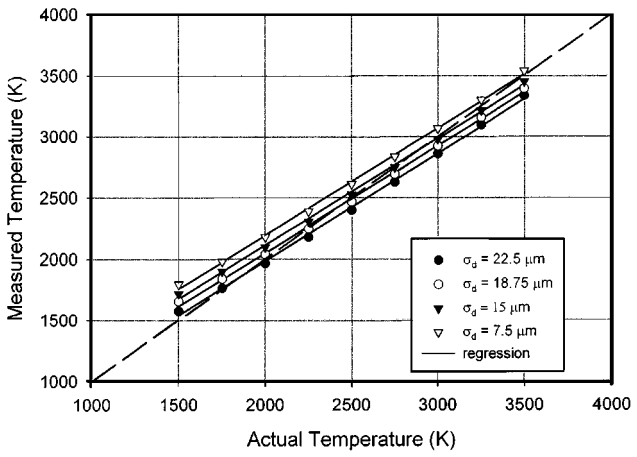

Fig. 15 Calculated pyrometer response to an ensemble of correlated particles, illustrating the effect of particle size distribution. The standard deviation in particle temperature is fixed at $\sigma_T = 300$ K and the temperature difference between the largest and smallest particles is 1200 K. The wavelength pairs are 950 nm and 1.35 μm

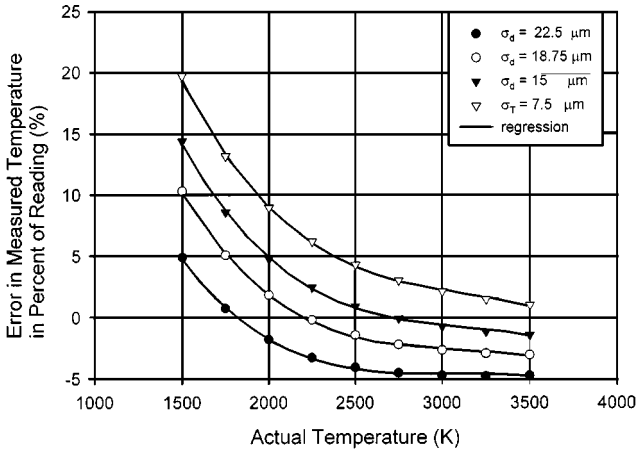

Fig. 16 Error in pyrometer response to an ensemble of correlated particles, illustrating the effect of particle size distribution. The standard deviation in particle temperature is fixed at $\sigma_T = 300$ K and the temperature difference between the largest and smallest particles is 1200 K. The wavelength pairs are 950 nm and 1.35 μm

particles. The larger the difference in temperature between the largest and smallest particles, the smaller is the error.

Figure 15 and 16 illustrate the effect of the width of the particle size distribution on pyrometer reading when particle temperature is correlated with particle size. The standard deviation of particle temperature is fixed at 300 °C and the width of the size distribution is varied as a parameter. The particle temperature is assumed to be strongly correlated with size and is assumed to change by 1200 °C between the largest (105 μm) and smallest (5 μm) particles. Narrow distributions of particle size result in consistent overprediction of temperature. At higher temperatures, a broader particle size distribution can reverse the trend and result in underprediction of temperature or a negative temperature error. In general, for particle ensemble temperatures on the order of 2000 K with distribution standard deviations of 300 °C or less, the errors are less than $<$10% of reading. For

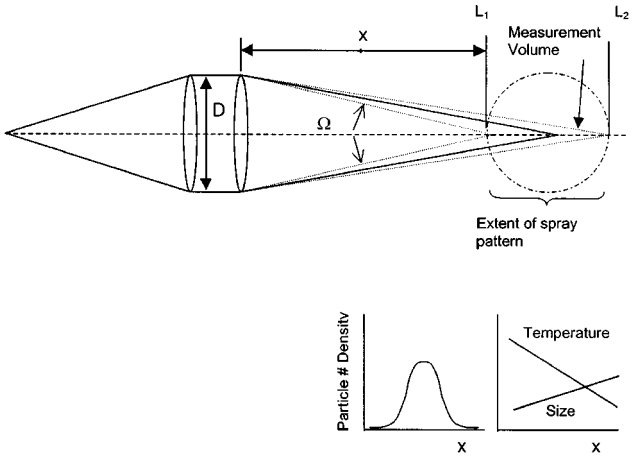

Fig. 17 Schematic of ensemble measurement technique optics and measurement volume

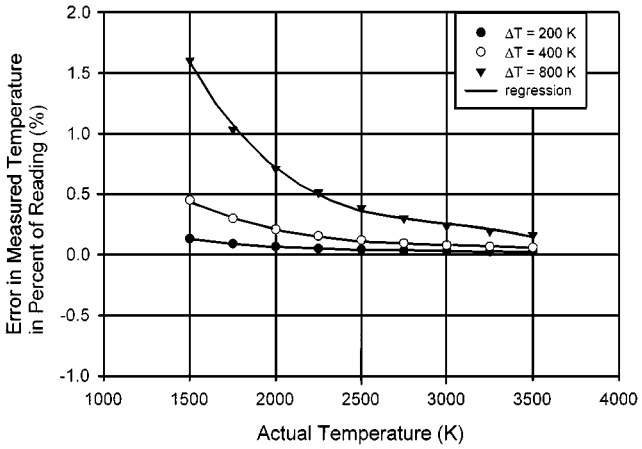

Fig. 18 Effect of the spatial distribution of particle temperature on ensemble pyrometer response

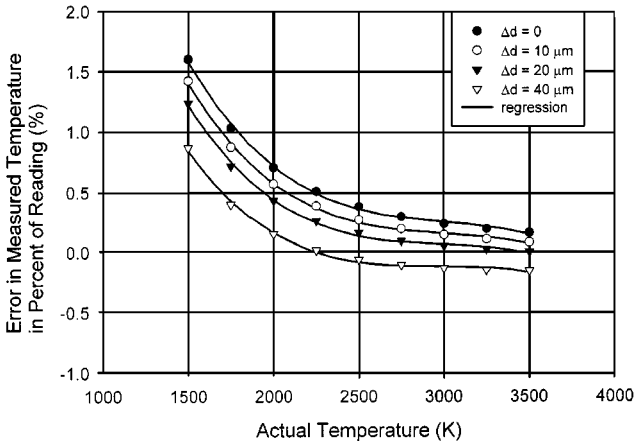

Fig. 19 Effect of the spatial distribution of particle size and temperature on ensemble pyrometer response

higher temperatures, on the order of the melting point of zirconia around 3000 K, for instance, the errors can be expected to fall in the range of ±5% of reading.

The final source of error that will be examined is illustrated Fig. 17. The ensemble temperature measurement technique implicitly averages over all particles in the measurement volume. The intensity contribution from each small disk-shaped slice or subregion to the total measured intensity will be a function of position, the statistical distribution of particle temperature and size, and the number of particles in the volume. The total intensity is found by integration over the extent of the measurement volume and over the particle size and temperature distribution. The total intensity for wavelength λ is given by

$$I_\lambda = \int_{L_1}^{L_2} \int_0^{d_{p\max}} \int_0^{T_{\max}} \frac{c_1 \varepsilon_\lambda \Delta\lambda \Omega(x) \frac{\pi d_p^2(x)}{4} N_p(x)}{\lambda^5 \left(e^{c_2/\lambda T} - 1\right)} f\left(T, d_p, x\right) dT\ dd_p\ dx_p$$

where $N_p(x)$ is the local relative particle number density. The functional form of the solid angle $\Omega(x)$ is

$$\Omega(x) = D^2/x^2$$

The spatial distribution of particle number density is assumed to be a Gaussian with standard deviation of 3.33 mm. This places 99% of the particles inside a spot size of ±10 mm, a size consistent with observations. Evaluation of the integral also requires that functional forms for the spatial distribution of particle temperature and size be specified. These are assumed to be linear with magnitudes that are consistent with observation.[1,2,27,28] In general, the particle size has been observed to vary by as much as a factor of 2 across the spray pattern, with the larger particles appearing the furthest from the injector. The particle temperature typically varies by a few hundred degrees across the pattern. For purposes of estimation, temperature differences of as much as 800 K have been assumed with the hottest particles nearest the injector. In the following, the particle size and temperature are assumed to vary with spatial position but are statistically uncorrelated with each other at a given spatial location. Exclusion of the temperature-diameter correlation results in a worst case estimate of error. It is also assumed that the particles are injected from left to right in Fig. 17. In this configuration, with the above assumptions, the hottest and smallest particles are nearest the light collection optics and, consequently, have the largest solid angle. A summary of the calculated temperature measurement error with temperature difference across the spray pattern treated as a parameter appears in Fig. 18. In developing this plot, it has been assumed that particle size is uniform across the spray pattern. For temperature differences of 400 K or less, the estimated temperature error is less than 0.5%. The effect of including the spatial distribution of particle size is shown in Fig. 19. Inclusion of size tends to suppress the estimated error slightly. This is because the particles nearest the light collection optics are hotter but are somewhat smaller in projected area, minimizing their weighting and reducing the resulting error. The temperature measurement error due to the spatial distribution of particle size and temperature is relatively small, on the order of 1% or less for most situations, which will be encountered in practice. The temperature measured is heavily weighted toward the largest particle density portion of the spray pattern. When the statistical distribution of particle temperature is included in the calculation,

its contribution to the error is much larger than the portion due to the spatial distribution of size and temperature alone. Because these results are essentially identical to the results of Fig. 11 and 12, they will not be illustrated here.

Summary

Measurement techniques can be categorized as single particle and ensemble methods. Single particle methods use high-speed pyrometry to estimate the temperature of individual particles. The mean and standard deviation of the particle temperature distribution can then be obtained from observations of sufficient numbers of individual particles. Ensemble methods observe large numbers of particles simultaneously and yield an estimated mean temperature directly, but cannot provide information on the shape or width of the particle temperature distribution. Each technique has inherent errors, strengths, and limitations.

Both techniques are susceptible to errors resulting from unknown or changing emissivity. The effect of emissivity can be large, resulting in errors in absolute temperature that can approach 20% in some cases. Both techniques suffer from stray light interference and must, in general, be applied at some distance from the bright plasma or combustion jet. Fortunately, at common standoff distances of 100 mm or so, the interference from stray light does not overwhelm either measurement; however, the lower limit of temperature that can be sensed is affected.

Single particle techniques require that the spray pattern be dilute enough that individual particles can be observed without overwhelming interference from nearby particles. This condition is met for many common thermal spray conditions. The measurement of single particle temperature is a statistical measurement. Sufficient data acquisition time must be allowed to acquire a statistically significant number of particles. Depending on the operating parameters and position in the spray pattern, this can take anywhere from a few seconds to a few minutes. Instrument noise artificially broadens the measured distribution of particle temperature. The magnitude of broadening depends on the situation, but something on the order of 100 K is common. Depending on the specifics of the instrument, other sources of statistical error can be present. These may not be normally distributed and can result in a bias as well as artificially broadening the measured temperature distribution. Because of the spatial distribution of temperature (profile) and the fact that the spray pattern is not spatially fixed, care must be exercised when applying the single particle temperature measurement technique to control or long-term monitoring applications.

The ensemble measurement technique is not limited to lightly loaded sprays and can be successfully applied to heavily loaded HVOF and high-powered plasma spray applications. The ensemble technique is insensitive to movement of the spray pattern and typically has a response time of 1 s or less. Ensemble measurement techniques, however, are influenced by the statistical distribution of particle temperature and size in the measurement volume. At temperatures on the order of 1500 K, this error can be large, on the order of 20%. At higher temperatures, on the order of 3000 K, this error is 5% or less. Ensemble techniques do not yield information of the distribution of particle temperatures.

Both techniques have application in the thermal spray industry. The single particle techniques yield additional information on the statistical distribution of particle temperature and are probably preferable for scientific investigation, but are somewhat more expensive, time consuming, and complicated to apply. Ensemble techniques are prone to absolute temperature measurement errors due to the statistical distribution of particle temperature in the measurement volume but are less expensive and insensitive to movement of the spray pattern. Insensitivity to spray pattern position, coupled with fast response times, makes ensemble techniques attractive for control applications.

Acknowledgments

This work was performed under the auspices of the U.S. Department of Energy under DOE Field Office, Idaho, Contract DE-AC07-99ID13727, supported by the U.S. Department of Energy, Office of Science, Office of Basic Energy Sciences, Division of Engineering and Geosciences.

References

1. J.R. Fincke, W.D. Swank, and C.L. Jeffery: *IEEE Trans. Plasma Sci.*, 1990, vol. 18, pp. 948-57.
2. J.R. Fincke, W.D. Swank, C.L. Jeffery, and C.A. Mancuso: *Measurement Sci. Technol.*, 1993, vol. 4, pp. 559-65.
3. C. Moreau, P. Gougeon, M. Lamontagne, V. Lacasse, G. Vaudreuil, and P. Cielo: in *Thermal Spray Industrial Applications*, C.C. Berndt and S. Sampath, eds., ASM International, Materials Park, OH, 1994, pp. 431-37.
4. C. Moreau, P. Gougeon, A. Burgess, and D. Ross: in *Thermal Spray Science and Technology*, C.C. Berndt and S. Sampath, eds., ASM International, Materials Park, OH, 1995, pp. 141–47.
5. M.A. Gurevich and V.B. Shetinberg: *Sov. Phys.-Tech. Phys.*, 1958, vol. 3, pp. 368-75.
6. B. Kruszewska and J. Lesinski: *Rev. Phys. Appl.*, 1977, vol. 12, pp. 1209-11.
7. A. Vardelle, J.M. Baronnet, M. Vardelle, and P. Fauchais: *IEEE Trans. Plasma Sci.*, 1980, vol. 8, pp. 418-24.
8. J. Mihsin, M. Vardelle, J. Lesinski, and P. Fauchais: *Proc. 7th Int. Plasma Chemistry*, IUPAC, Eindhoven, 1985, pp. 724-29.
9. J. Mihsin, M. Vardelle, J. Lesinski, and P. Fauchais: *J. Phys. E: Scientific Instrumentation*, 1987, vol. 20, pp. 620-25.
10. F.R.A. Jorgensen and M. Zuiderwyk: *J. Phys. E: Scientific Instrumentation*, 1985, vol. 18, pp. 486-91.
11. M. Vardelle, A. Vardelle, P. Fauchais, and M.I. Boulous: *J. AICE*, 1983, vol. 29, pp. 236-43.
12. J. Fincke, C.L. Jeffery, and S.B. Englert: *J. Phys. E: Sci. Instrum.*, 1988, vol. 21, pp. 367-70.
13. D.A. Tichenor, R.E. Mitchell, K.R. Hencken, and S. Niksa: "Simultaneous *In Situ* Measurement of the Size, Temperature and Velocity of Particles in a Combustion Environment," Report No. SAND 84-8628, Sandia National Laboratory, Albuquerque, NM, 1984.
14. T. Sakuta and M.I. Boulos: *Proc. 8th Int. Plasma Chem.*, IUPAC, Tokyo, 1987, pp. 371-77.
15. T. Sakuta and M.I. Boulos: *Rev. Sci. Instrum.*, 1988, vol. 59, pp. 285-91.
16. H. Hantzsche: *7th Int. Metal Spraying Conf.*, London, Sept. 10-14, 1973, Edison Welding Institute, Columbus, OH, 1973, pp. 1-4.
17. X. Xu, G. Chen, and Y. Shen: 1st Plasma-Technik-Symp., Lucerne, May 18–20, 1988, Plasma-Technik, 1988, pp. 99–103.
18. S. Kuroda, T. Fukushima, S. Kitahara, and H. Fujimori: *12th Int. Conf. Thermal Spraying*, London, June 4–9, 1989, The Welding Institute, Abington, United Kingdom, 1989, pp. 145-53.

19. W.D. Swank, J.R. Fincke, and D.C. Haggard: *Thermal Spray Science and Technology*, C.C. Berndt and S. Sampath, eds., ASM International, Materials Park, OH, 1995, pp. 111-16.
20. J.R. Fincke, W.D. Swank, and D.C. Haggard: in *Thermal Spray Science and Technology*, C. Berndt and S. Sampath, eds., ASM International, Materials Park, OH, 1995, pp. 117-22.
21. J.R. Fincke, W.D. Swank, and D.C. Haggard: *Thermal Spray Science and Technology*, C.C. Berndt and S. Sampath, eds., ASM International, Materials Park, OH, 1995, pp.123-28.
22. P. Gougeon and C. Moreau: in *Thermal Spray Coating: Research, Design, and Applications*, C. Berndt and T. Bernecki, eds., ASM International, Materials Park, OH, Anaheim, CA, 1993.
23. J.C. De Vos: *Physica*, 1954, vol. XX, pp. 690-714.
24. Y. S. Touloukian and D. P. Dewitt: *Thermal Radiative Properties of Metallic Elements and Alloys*, IFI/Plenum, New York, NY, 1970, vol. 7.
25. Y.S. Touloukian and D.P. Dewitt: *Thermal Radiative Properties of Nonmetallic Solids*, IFI/Plenum, New York, NY, 1972, vol. 8.
26. R.L. Williamson, J.R. Fincke, and C.H. Chang: *Plasma Chem. Plasma Processing*, 2000, vol. 20, pp. 299-323.
27. P. Gougeon, C. Moreau, and F. Richard: in *Thermal Spray Science and Technology*, C.C. Berndt and S. Sampath, eds., ASM International, Materials Park, OH, 1995, pp. 149-55.
28. A. Vardelle, J.M. Baronnet, M. Vardelle, and P. Fauchais: *IEEE Trans. Plasma Sci.*, 1980, vol. PS-8, pp. 417-24.